

Communication

A Benzimidazolium-Based Organic Cage with Antimicrobial Activity

Sonia La Cognata ¹, Donatella Armentano ², Nicoletta Marchesi ³, Pietro Grisoli ³, Alessia Pascale ³, Marion Kieffer ⁴, Angelo Taglietti ¹, Anthony P. Davis ⁴ and Valeria Amendola ^{1,*}

¹ Department of Chemistry, University of Pavia, Viale Torquato Taramelli 12, 27100 Pavia, Italy

² Department of Chemistry & Chemical Technologies, University of Calabria, Via P. Bucci 14/C, 87036 Rende, Italy

³ Department of Drug Sciences, Section of Pharmacology, University of Pavia, Viale Torquato Taramelli 12, 27100 Pavia, Italy

⁴ School of Chemistry, University of Bristol, Bristol BS8 1TS, UK

* Correspondence: valeria.amendola@unipv.it

Abstract: Considering the wide interest in (benz)imidazolium-based drugs, we here report our study on a benzimidazolium-based organic cage as potential antimicrobial and antifungal agent. Cytotoxicity studies on a human derived cell line, SH-SY5Y, showed that the cage is not cytotoxic at all at the investigated concentrations. Anion binding studies demonstrated that the cage can bind anions (chloride and nitrate, in particular) both in organic solvent and 20%v D₂O/CD₃CN mixture. The cage was also tested as anionophore, showing a weak but measurable transport of chloride and nitrate across LUVs vesicles. Nonetheless, the compounds have antimicrobial activity towards *Staphylococcus aureus* (Gram-positive bacteria). This is probably the first organic cage studied as anionophore and antimicrobial agent.

Keywords: organic cage; anion binding; anion transport; imidazolium-based receptor; antimicrobial activity



Citation: La Cognata, S.; Armentano, D.; Marchesi, N.; Grisoli, P.; Pascale, A.; Kieffer, M.; Taglietti, A.; Davis, A.P.; Amendola, V. A

Benzimidazolium-Based Organic Cage with Antimicrobial Activity. *Chemistry* **2022**, *4*, 855–864. <https://doi.org/10.3390/chemistry4030061>

Academic Editor: Robert B. P. Elmes

Received: 30 July 2022

Accepted: 23 August 2022

Published: 26 August 2022

Publisher's Note: MDPI stays neutral with regard to jurisdictional claims in published maps and institutional affiliations.



Copyright: © 2022 by the authors. Licensee MDPI, Basel, Switzerland. This article is an open access article distributed under the terms and conditions of the Creative Commons Attribution (CC BY) license (<https://creativecommons.org/licenses/by/4.0/>).

1. Introduction

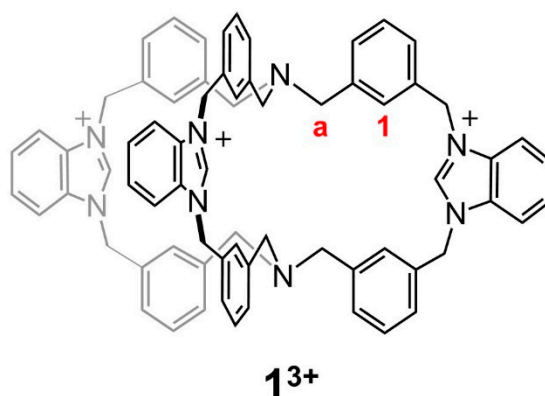
Over the last decades, anion receptors have raised great interest for applications in e.g., molecular recognition and sensing, [1–4] extraction and separation processes, [5–7] transport across membranes [8–10]. This latter application is particularly relevant in the biomedical field, considering the number of pathologies connected to disfunctions of natural anion channels or related to anomalies in transmembrane anion transport processes [11–13]. Among molecular receptors, cage-like hosts are of particular interest because their cavity can be designed for the selective encapsulation of target guests, [14] such as relevant biological anions. Once encapsulated in the cage's cavity, the anion can be transported through biological membranes, being protected by the cage skeleton from the attacks from enzymes or other reactive species [15–17]. This feature makes cage-like compounds suitable candidates for future applications, including the development of drugs [16]. In this work, we evaluated the potential application of a benzimidazolium organic cage as anion transporter and antimicrobial agent.

The possibility to exploit anion transporters to generate imbalances of anion concentration across the cell membranes is considered promising for the development of new antimicrobial drugs. Within this context, imidazolium and benzimidazolium salts have shown promising results as ionophores, being capable of generating anion imbalances in living microorganisms [18]. Tests on model membrane liposomes, as well as membrane depolarization studies and scanning electron microscopy on living bacteria, showed that the action of (benz)imidazolium-based antimicrobials is connected to the destabilization of bacterial membrane [19,20]. The high antimicrobial effect observed with Gram-positive

bacteria, as compared to Gram-negative ones, was attributed to the different composition of the bacterial membrane. In particular, the double layer of phospholipids, which constitutes the membrane of Gram-negative bacteria, can offer a better resistance to this type of anionophore [8,17,20,21]. Most of the proposed benzimidazolium-based antimicrobials showed minimal inhibitory concentrations and low cytotoxicity towards human cells. However, the toxicity of some imidazolium salts was considered useful for different applications, such as the development of antitumoral drugs [11,22] or antifungal agents.

Among molecular hosts, imidazolium-based systems have attracted considerable attention as anion receptors, due to the strong H-donor tendencies of the (C-H)⁺ bond [23–30]. The arrangement of multiple C–H donors, such as imidazolium groups, around the cavity of bowl-shaped receptors, macrocycles, or cages, can generate a synergistic effect that increases the receptor's affinity towards target anionic guests. This strategy can lead to the selective binding of anions in competing media, including organic-water mixtures (e.g., acetonitrile/water 4/1, *v/v*) [24].

A few years ago, our group investigated the hexafluorophosphate salt of a tris (imidazolium)-based organic cage, as a receptor for halides in both pure acetonitrile and acetonitrile/water (98/2, *v/v*) mixture [31]. These studies showed that the cage had a strong affinity for chloride, and that the binding of this anion was accompanied by a significant rearrangement of the cage conformation. A similar chloride-induced conformational change was hypothesized for the tris (benzimidazolium)-based analogue, i.e., **1**³⁺ (Scheme 1).



Scheme 1. Structure of the organic cage **1**³⁺. In this work we investigated the properties of both **1**(PF₆)₃ and **1**(NO₃)₃ compounds. Positions of the relevant protons Ha and H1 are indicated in red.

In this work, we focused on the **1**³⁺ receptor, that was isolated as both hexafluorophosphate and nitrate salts, i.e., **1**(PF₆)₃ and **1**(NO₃)₃. Synchrotron X-ray diffraction studies on single crystals of **1**(PF₆)₃ allowed us to determine the cage structure. The affinity of **1**³⁺ for the nitrate anion was then investigated on **1**(PF₆)₃ by titration in pure acetonitrile. The binding of chloride was instead investigated in a more competing medium (i.e., 20%v D₂O/CD₃CN) using **1**(NO₃)₃ for the titration with the anion. Considering the wide interest in (benz)imidazolium-based drugs, we performed a series of experiments on **1**(PF₆)₃ and **1**(NO₃)₃ to test the cytotoxicity of these compounds, and their potential application as antifungal and antibacterial agents. Preliminary investigations on **1**(NO₃)₃ as anion transporter across membranes were also performed.

2. Materials and Methods

The **1**(PF₆)₃ compound was prepared using a procedure already described by our group [31]. **1**(PF₆)₃ has a good solubility in acetonitrile (5 mM), but a low solubility in water (<0.1 mM). The solubility in aqueous solution was increased (up to 0.01 M) using nitrate as counterion. The **1**(NO₃)₃ compound was prepared from the corresponding bromide salt by anion exchange. Details on preparation and characterization of **1**(NO₃)₃ are reported

in the S.I. Experimental details on single crystals X-ray diffraction analysis, UV-vis. and NMR titrations and characterization, cytotoxicity, antifungal and antimicrobial tests, anion transport studies are available in the Supplementary Information.

3. Results and Discussion

3.1. Crystals of $1(\text{PF}_6)_3$

Single crystals of $1(\text{PF}_6)_3$ were obtained by slow diffusion of diethyl ether into an acetonitrile solution of the compound. The structural investigation through Synchrotron X-ray diffraction (SCXRD) revealed that the cage molecule assumes a flattened conformation like that observed in the trisimidazolium analogue [31]. The tertiary amines point their lone pair outside the cage, and the separation between the N_{tert} atoms measures 6.06 Å. In this conformation, the positively charged arms extend apart, minimizing electrostatic repulsions. With respect to the imidazolium-based system, the tribenzylamines are not eclipsed, and there is no symmetry plane dividing the molecule. On the contrary, the tribenzylamine-based platforms are almost staggered (dihedral angles between 60° and 67°), and twisted in opposite directions (i.e., clockwise/counter-clockwise). In the crystal structure of $1(\text{PF}_6)_3$, the cage cavity seems empty. Hence, the counter-anions are located outside the cage, interacting with $\text{C}_{\text{aryl}}\text{-H}$ and $(\text{C-H})^+$ H-donors of the benzimidazolium-containing arms.

Indeed, the cage assumes an almost flattened conformation. However, looking more in depth at its crystal structure, it is evident how the conformation of the cage allows cooperative host-guest interactions of the type $\text{C-H}\cdots\text{F}$ with $\text{C}\cdots\text{F}$ distances ranging from 3.12 to 3.69 Å. Figure 1 shows PF_6^- anions anchored on the narrow window of the cage. Likely, the short separation between the N_{tert} atoms (of 6.06 Å) and the consequent small virtual diameter is not enough to allow the inclusion of PF_6^- anions, hosted and stabilized by weak interactions in the most accessible pocket (Figure S5).

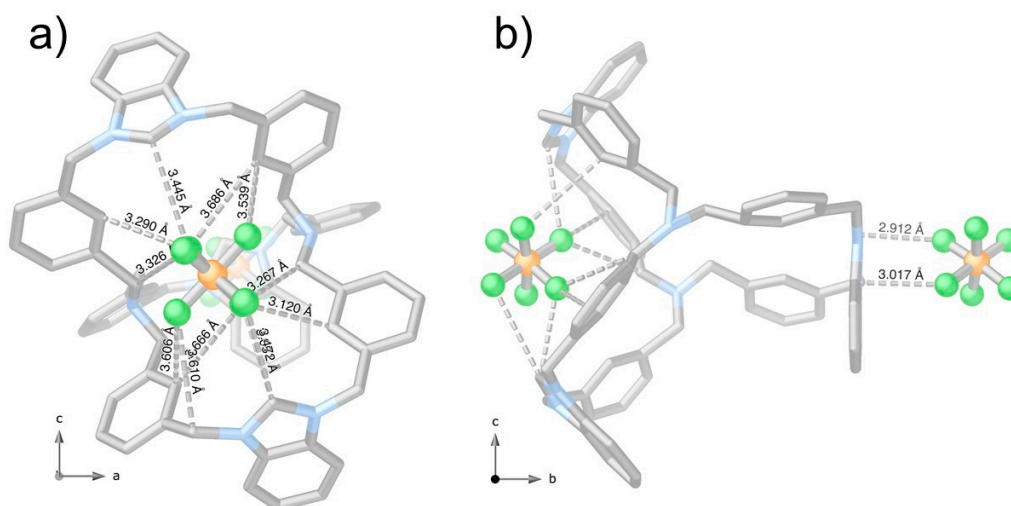


Figure 1. Crystal structure of $1(\text{PF}_6)_3$ along b and a crystallographic axes, see subfigures (a,b), respectively. Hydrogen atoms and one of the three PF_6^- counterions have been omitted for clarity.

3.2. Spectroscopic Studies on 1^{3+} with Anions

The NMR characterization of $1(\text{PF}_6)_3$ in pure CD_3CN and, in particular, the chemical shifts of $\text{C}_{\text{aryl}}\text{-H}$ and $(\text{C-H})^+$ protons in the $^1\text{H-NMR}$ spectrum (i.e., H1 and Ha, respectively, in Figure S3) suggest that the hexafluorophosphate anion stays outside the cavity. We can hypothesize that the cage assumes a flattened conformation like that in the crystalline state (as also found for the imidazolium-based system), with the benzimidazolium groups oriented far from each other, to minimize electrostatic repulsions.

On the other hand, the $^1\text{H-NMR}$ spectrum of $1(\text{NO}_3)_3$ in pure CD_3CN indicates the presence of H-bonding interactions between the 1^{3+} cage and nitrate (see Figure S6). In fact,

the peaks of $C_{\text{aryl}}\text{-H}$ and $(\text{C-H})^+$ protons are significantly downfield shifted compared to the spectrum of $1(\text{PF}_6)_3$. In addition, $^1\text{H-NMR}$ and NOESY spectra resemble those recorded on the 1:1 complex of the imidazolium-based analogue cage with chloride [31]. These observations are consistent with the hypothesis that at least one of the nitrate anions [of the $1(\text{NO}_3)_3$ salt] is strongly bound by the receptor, involving $C_{\text{aryl}}\text{-H}$ and $(\text{C-H})^+$ in the binding. As expected, if D_2O is added into the NMR tube, the peaks of $C_{\text{aryl}}\text{-H}$ and $(\text{C-H})^+$ protons shift towards the positions observed in $1(\text{PF}_6)_3$, suggesting that in $\text{CD}_3\text{CN}/\text{D}_2\text{O}$ mixture the interaction of nitrate with the cavity is weakened. However, the overall results indicate that nitrate can compete with chloride in the binding of the cage.

The formation of a stable 1:1 complex between 1^{3+} and nitrate, in pure acetonitrile, was confirmed by the UV-vis titration of $1(\text{PF}_6)_3$ with tetrabutylammonium nitrate, i.e., $[\text{TBA}]\text{NO}_3$. As shown in Figure 2, the anion binding promotes small but significant shifts of the UV-vis. bands of the receptor. These shifts, which are attributable to an effect of the binding on the electronic transitions of benzimidazolium units, are in line with those observed in our previous study [31] under UV-vis. titrations of 1^{3+} with bromide and chloride ($\log K_{11} = 5.8(1)$ and $\log K_{11} > 6$, respectively). The titration data were processed with the Hyperquad package [32] to determine the equilibrium constants. The bestfit was obtained considering a 1:1 host:guest binding stoichiometry with an association constant of 5.3(1) log units.

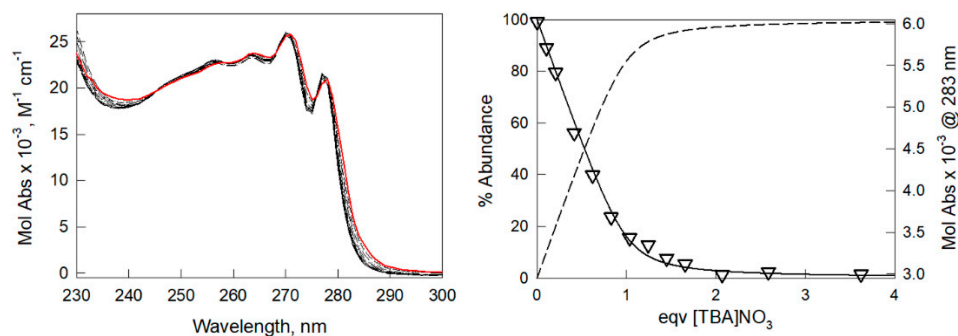


Figure 2. UV-vis. titration of a solution of $1(\text{PF}_6)_3$ (0.174 mM) in acetonitrile with a 100-fold more concentrated solution of $[\text{TBA}]\text{NO}_3$. On the left: family of spectra taken during titration (red line and black solid lines: initial and final spectra, respectively). On the right: distribution diagram of the species, calculated for an association constant of 5.3 log units (solid line: % of the free 1^{3+} cage; dashed line: % of 1:1 complex with nitrate, $[1(\text{NO}_3)]^{2+}$, with the superimposed experimental data (triangles) of the Molar Absorptivity at 283 nm (right-hand y-axis) vs. eqv. of $[\text{TBA}]\text{NO}_3$. The distribution diagram was obtained using the Hyss software (Hyperquad package) [32].

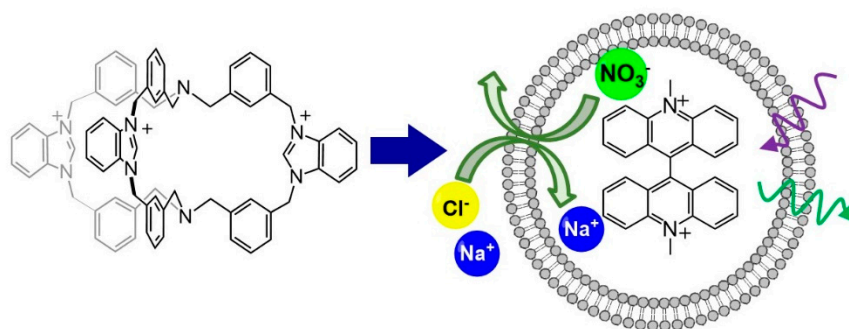
We also investigated the capability of the 1^{3+} cage to bind the chloride anion in $\text{CD}_3\text{CN}/\text{D}_2\text{O}$, 4/1 *v/v*, mixture. Due to the low solubility of $1(\text{PF}_6)_3$ in this medium, the $1(\text{NO}_3)_3$ salt was employed for the study (Figures S7 and S8). Notably, the addition of standard $[\text{TBA}]\text{Cl}$ to the receptor's solution was accompanied by a significant downfield shift of the $C_{\text{aryl}}\text{-H}$ peaks. This result is consistent with the involvement of the aryl protons in the binding of chloride within the cavity. Titration data were processed with the Hyperquad package [32]; also in this case the best-fit was obtained considering a 1:1 binding stoichiometry. The binding constant measures 1.53(2) log units. This low value is not surprising, considering the high percentage of D_2O in the mixture (20%v), and the presence of competing anions (i.e., 3 eqv. of nitrate) in solution. The NOESY spectrum, recorded under addition of excess $[\text{TBA}]\text{Cl}$ (i.e., 30:1 $\text{Cl}^-:1^{3+}$, 10:1 $\text{Cl}^-:\text{NO}_3^-$ molar ratios), suggested that chloride binding promotes the conformational rearrangement of the cage. Notably, the correlation between H1 and Ha protons (see Figures S9 and S11), observable in the NOESY spectrum of $1(\text{NO}_3)_3$, almost disappeared under excess chloride. This indicates that the anion stabilizes a conformation of the cage, in which the separation of H1 and Ha protons has increased. Comparable results were observed for the complex of

the imidazolium-based system: chloride binding within the cage's cavity promoted an elongation of the cage, accompanied by the pyramidal inversion of the tertiary amines [31]. This conformational rearrangement allowed the (C–H)⁺ groups to point towards the centre of the cavity and cooperate in the binding of the anionic guest [24,25,31,33–35]. We can hypothesize a similar rearrangement in our case.

Considering the binding ability of the cage towards anions, we wanted to check whether the receptor could be also employed as an anion transporter across membranes. These studies can be relevant for the potential biological application of the tris-benzimidazolium cage.

3.3. Anion Transport Studies

The antimicrobial activity of imidazolium and benzimidazolium salts is generally related to the tendency of these compounds to act as anionophores, capable of generating imbalances of anion concentration across the cell membranes of living microorganisms. The ability of **1**³⁺ to act as an anionophore, promoting anion transport across bilayer membranes, was studied in large unilamellar vesicles (LUVs) employing the methodology previously reported by the Bristol group [21,36,37]. LUVs are prepared from a 7:3 mixture of 1-Palmitoyl-2-oleoyl-sn-glycero-3-phosphocholine (POPC) and cholesterol by extrusion through a polycarbonate membrane (200 nm), with sodium nitrate and the halide-sensitive fluorescent dye lucigenin in the aqueous phase. The potential anionophore may be added to the vesicle lipids prior to extrusion (preincorporation method) or added later (external addition). Sodium chloride is added to the exterior solution to start the transport experiment, and chloride influx is followed by monitoring the decrease in lucigenin emission caused by quenching. Assuming no cation transport, the chloride influx must be accompanied by nitrate efflux to maintain electroneutrality (see Scheme 2).



Scheme 2. Anion transport experiment with the **1**³⁺ cage.

Experiments involving external addition of **1**(NO₃)₃, dissolved in a small amount of methanol, yielded negative results. However, when **1**(NO₃)₃ was preincorporated in the LUVs at a mole ratio of transporter:lipid:1:2500, anion transport was detected. The rates were very low in the context of previously published work, but measurable and reproducible. Traces from both types of experiment are reproduced in Figure S11. It thus seems that **1**(NO₃)₃ is able to transport both chloride and nitrate across the vesicle membranes, albeit slowly, but is not capable of finding and/or inserting into the membranes if added externally under the conditions of these experiments.

The poor performance of **1**³⁺ as anionophore, compared to other (benz)imidazolium-based systems, can be due to the presence of three positive charges, that increase the hydrophilicity (at the expense of lipophilicity) impairing the ability of the cage to enter the membrane. In fact, the best results described in the literature were obtained with molecules presenting a better hydrophilicity/hydrophobicity balance [20,38]. Nonetheless, considering the wide interest in imidazolium salts as drugs, we decided to proceed with the study on the antimicrobial and antifungal properties of **1**(PF₆)₃ and **1**(NO₃)₃ compounds.

3.4. Antimicrobial and Antifungal Investigations on $1(\text{PF}_6)_3$ and $1(\text{NO}_3)_3$

Before studying the potential application of 1^{3+} as antibacterial and/or antifungal agent, we verified the potential cytotoxicity of $1(\text{PF}_6)_3$ and $1(\text{NO}_3)_3$ on SH-SY5Y, a human derived cell line. SH-SY5Y cells are commonly employed as a human model of eukaryotic cells, besides they are also widely used as a neuronal-like cellular model [39,40].

The effect of $1(\text{PF}_6)_3$ and $1(\text{NO}_3)_3$ was tested on the mitochondrial activity of SH-SY5Y cells, using different concentrations of imidazolium salt (100 nM, 1 μM , 10 μM , 100 μM) for 24 h and 48 h. Notably, under the adopted experimental conditions, both salts were found to be safe at all the assayed concentrations and times of exposure (Figure 3). Although minimal variations were observed in comparison to the control group (100%), all the values were above the “biocompatibility” threshold, which is set at 70% [41].

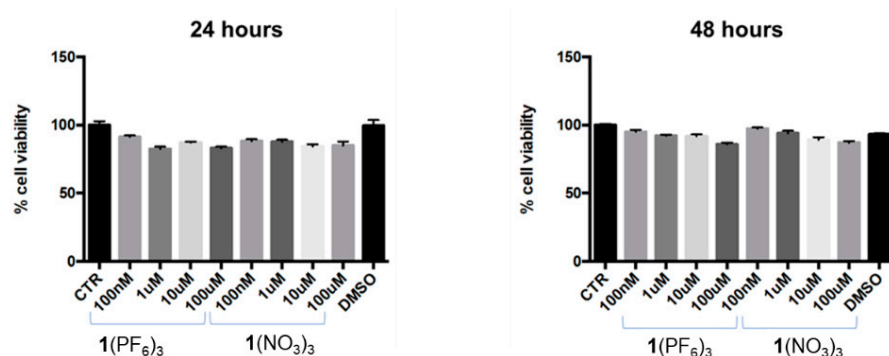


Figure 3. Effect of $1(\text{PF}_6)_3$ and $1(\text{NO}_3)_3$ salts on mitochondrial activity in SH-SY5Y cells. Cells were exposed to different concentrations of $1(\text{PF}_6)_3$ and $1(\text{NO}_3)_3$ for 24 h and 48 h. Absorbance values obtained after the MTT assay are expressed as mean percentages \pm S.E.M. over controls (CTR, 100%), $n = 8$. CTR = control; DMSO (solvent) = dimethyl sulfoxide.

The cage compounds $1(\text{NO}_3)_3$ and $1(\text{PF}_6)_3$ were then evaluated against different microbial strains: *Staphylococcus aureus* (Gram-positive bacteria), *Escherichia coli* (Gram-negative bacteria) and *Candida albicans* (yeast).

Table 1 shows antimicrobial concentrations (MIC/MBC/MFC, $\mu\text{g}/\text{mL}$), determined by means of the standard serial dilution method, according to NCCLS (see the S.I. for details) [42,43]. Two available antimicrobial drugs, ampicillin and amphotericin B, were used as positive controls. The assayed microbial strains show a different sensitivity in the antimicrobial tests. Both salts show greater activity on *S. aureus* than against the other microorganisms [44,45]. In particular, $1(\text{NO}_3)_3$ is the most effective compound against the three microorganisms and among bacteria has the lowest MIC and MBC values on *S. aureus*: 15.82 $\mu\text{g}/\text{mL}$ (13.29 μM) and 190.00 $\mu\text{g}/\text{mL}$ (160 μM), respectively. The corresponding MIC and MBC values on *S. aureus* obtained for $1(\text{PF}_6)_3$ were 31.45 $\mu\text{g}/\text{mL}$ (corresponding to 21.85 μM concentration) and 255 $\mu\text{g}/\text{mL}$ (177 μM). The effect on *C. albicans* is the least intense for $1(\text{NO}_3)_3$ with the MIC equal to 210.00 $\mu\text{g}/\text{mL}$ (176 μM). The greater susceptibility of *S. aureus* derives from the different structure and composition of the cell wall compared to other microorganisms. In particular, as the Gram-positive cell has a thicker wall, made up of 90% peptidoglycan; [44] on the other hand, the Gram-negative bacterium *E. coli* has a thinner wall, equipped with a consistent lipid, liposaccharide and protein component in the external part of the cell wall, called outer membrane [46]. The *E. coli* cell wall is thus more lipophilic than the wall of *S. aureus* [47]: the highly charged cage is expected to interact more easily with the less hydrophobic wall of the latter, and this can explain the higher microbicidal action of the cage towards the Gram-positive strain. Fungi such as *Candida albicans* have a different wall than those observed in bacteria, containing polysaccharides, lipids, and proteins, which in general make it less sensitive to the action of biocides [48–50]. Therefore, the structure of the microbial cell envelope can affect the spread of harmful compounds [38]. In fact, the presence of an external membrane

in Gram-negative bacteria and the other differences described in the composition of fungi cell wall, make these microorganisms less permeable to the salts tested, confirming the greater effectiveness of these compounds on Gram-positive bacteria [18].

Table 1. MIC (minimum inhibitory concentration) and MBC/MFC (minimum bactericidal/fungicidal concentration) values ¹ of cage compounds against *Staphylococcus aureus*, *Escherichia coli* and *Candida albicans*.

Microorganisms	1(NO₃)₃		1(PF₆)₃		Amp-Amph ²	
	MIC	MBC/MFC μg/mL	MIC	MBC/MFC μg/mL	MIC	MBC/MFC μg/mL
<i>Staphylococcus aureus</i> ATCC 6538	15.82	190.00	31.45	255.00	0.50	1.00
<i>Escherichia coli</i> ATCC 10646	127.50	250.00	250.00	>255.00	5.00	10.00
<i>Candida albicans</i> ATCC 10231	210.00	>255.00	255.00	>255.00	0.50	2.00

¹ Values are obtained as the average of three measurements. ² Amp-Amph: ampicillin, amphotericin B, antibiotic control.

4. Conclusions

In this paper, we extended a previous investigation on the 1³⁺ cage, reporting the crystal structure of the free cage (as hexafluorophosphate salt), and the anion binding ability towards nitrate and chloride. The cage was also tested as anionophore, showing a weak but measurable transport of chloride and nitrate across LUVs vesicles. The presence of three positively charges probably increases the hydrophilicity of the cage, thus negatively affecting the ability to enter the membrane. Nonetheless, our compounds showed antimicrobial activity towards *Staphylococcus aureus* (Gram-positive bacterium). The effect on Gram-positive bacteria, compared to Gram-negative bacteria and fungi, is due to the different structure of the cell membrane and wall. 1(NO₃)₃ was found to be the most effective compound showing the lowest MIC and MBC values on *S. aureus*. Further investigations will be performed to (i) elucidate the mechanism of the antimicrobial activity, (ii) evaluate the effect of other counterions on the activities the corresponding salts, (iii) improve the hydrophilicity/hydrophobicity balance of the cage structure, in order to enhance its ability to enter the membrane. As far as we know, this is the first organic cage studied as anionophore and antimicrobial agent.

Supplementary Materials: The following supporting information can be downloaded at: <https://www.mdpi.com/article/10.3390/chemistry4030061/s1>. Details on Materials and Methods; Synthesis and characterization of 1(NO₃)₃ (ESI-MS and NMR spectra); supplementary information on SCXRD analysis, ¹H-NMR titrations with chloride, NOESY spectra, anion transport studies. References [50–59] are cited in supplementary materials.

Author Contributions: Investigation, S.L.C., P.G., D.A., N.M., M.K.; resources, P.G., A.P., A.P.D.; writing—original draft preparation, V.A.; writing—review and editing, V.A., A.T.; supervision, V.A., A.P.D., A.P.; project administration, V.A.; funding acquisition, V.A., D.A. All authors have read and agreed to the published version of the manuscript.

Funding: The Italian Ministry of Education, Universities and Research and the University of Pavia are acknowledged for funding.

Institutional Review Board Statement: Not applicable.

Informed Consent Statement: Not applicable.

Data Availability Statement: The data that support the findings of this study have been deposited in the CCDC database with reference number 2193392.

Acknowledgments: Teresa Recca and Barbara Mannucci of the Centro Grandi Strumenti (University of Pavia) are gratefully thanked for instrumental support. D.A. particularly acknowledges the

Diamond Light Source for the awarded beamtime and provision of synchrotron radiation facilities (proposal no. CY22411-1) and Dr David Allan and Sarah Barnett for their assistance at the I19 beamline. APD and MK acknowledge support from the UK Medical Research Council [grant number MR/S00274X/1].

Conflicts of Interest: The authors declare no conflict of interest.

References

1. Aletti, A.B.; Gillen, D.M.; Gunnlaugsson, T. Luminescent/colorimetric probes and (chemo-) sensors for detecting anions based on transition and lanthanide ion receptor/binding complexes. *Coord. Chem. Rev.* **2018**, *354*, 98–120. [[CrossRef](#)]
2. McNaughton, D.A.; Fares, M.; Picci, G.; Gale, P.A.; Caltagirone, C. Advances in fluorescent and colorimetric sensors for anionic species. *Coord. Chem. Rev.* **2021**, *427*, 213573. [[CrossRef](#)]
3. Mako, T.L.; Racicot, J.M.; Levine, M. Supramolecular Luminescent Sensors. *Chem. Rev.* **2018**, *119*, 322–477. [[CrossRef](#)] [[PubMed](#)]
4. Amendola, V.; Bergamaschi, G.; Miljkovic, A. Azacryptands as molecular cages for anions and metal ions. *Supramol. Chem.* **2018**, *30*, 236–242. [[CrossRef](#)]
5. Liu, Y.; Sengupta, A.; Raghavachari, K.; Flood, A.H. Anion Binding in Solution: Beyond the Electrostatic Regime. *Chem* **2017**, *3*, 411–427. [[CrossRef](#)]
6. Liu, Y.; Zhao, W.; Chen, C.H.; Flood, A.H. Chloride capture using a C–H hydrogen bonding cage. *Science* **2019**, *365*, 159–161. [[CrossRef](#)]
7. La Cognata, S.; Mobili, R.; Merlo, F.; Speltini, A.; Boiocchi, M.; Recca, T.; Maher, L.J.; Amendola, V. Sensing and Liquid-Liquid Extraction of Dicarboxylates Using Dicopper Cryptates. *ACS Omega* **2020**, *5*, 26573–26582. [[CrossRef](#)]
8. Wu, X.; Howe, E.N.W.; Gale, P.A. Supramolecular Transmembrane Anion Transport: New Assays and Insights. *Acc. Chem. Res.* **2018**, *51*, 1870–1879. [[CrossRef](#)]
9. Bickerton, L.E.; Johnson, T.G.; Kerckhoffs, A.; Langton, M.J. Supramolecular chemistry in lipid bilayer membranes. *Chem. Sci.* **2021**, *12*, 11252–11274. [[CrossRef](#)]
10. Mondal, D.; Ahmad, M.; Panwaria, P.; Upadhyay, A.; Talukdar, P. Anion Recognition through Multivalent C–H Hydrogen Bonds: Anion-Induced Foldamer Formation and Transport across Phospholipid Membranes. *J. Org. Chem.* **2022**, *87*, 10–17. [[CrossRef](#)]
11. Gale, P.A.; Davis, J.T.; Quesada, R. Anion transport and supramolecular medicinal chemistry. *Chem. Soc. Rev.* **2017**, *46*, 2497–2519. [[CrossRef](#)] [[PubMed](#)]
12. Gale, P.A.; Pérez-Tomás, R.; Quesada, R. Anion transporters and biological systems. *Acc. Chem. Res.* **2013**, *46*, 2801–2813. [[CrossRef](#)] [[PubMed](#)]
13. Picci, G.; Kubicki, M.; Garau, A.; Lippolis, V.; Mocci, R.; Porcheddu, A.; Quesada, R.; Ricci, P.C.; Scorciapino, M.A.; Caltagirone, C. Simple squaramide receptors for highly efficient anion binding in aqueous media and transmembrane transport. *Chem. Commun.* **2020**, *56*, 11066–11069. [[CrossRef](#)] [[PubMed](#)]
14. Amendola, V.; Alberti, G.; Bergamaschi, G.; Biesuz, R.; Boiocchi, M.; Ferrito, S.; Schmidtchen, F.-P. Cavity Effect on Perrhenate Recognition by Polyammonium Cages. *Eur. J. Inorg. Chem.* **2012**, *2012*, 3410–3417. [[CrossRef](#)]
15. Tapia, L.; Alfonso, I.; Solà, J. Molecular cages for biological applications. *Org. Biomol. Chem.* **2021**, *19*, 9527–9540. [[CrossRef](#)]
16. Tapia, L.; Pérez, Y.; Bolte, M.; Casas, J.; Solà, J.; Quesada, R.; Alfonso, I. pH-Dependent Chloride Transport by Pseudopeptidic Cages for the Selective Killing of Cancer Cells in Acidic Microenvironments. *Angew. Chem. Int. Ed.* **2019**, *58*, 12465–12468. [[CrossRef](#)]
17. Gravel, J.; Schmitzer, A.R. Imidazolium and benzimidazolium-containing compounds: From simple toxic salts to highly bioactive drugs. *Org. Biomol. Chem.* **2017**, *15*, 1051–1071. [[CrossRef](#)]
18. Vidal, M.; Elie, C.R.; Campbell, S.; Claing, A.; Schmitzer, A.R. Biologically active binaphthol-scaffolded imidazolium salts. *MedChemComm* **2014**, *5*, 436–440. [[CrossRef](#)]
19. Elie, C.R.; David, G.; Schmitzer, A.R. Strong antibacterial properties of anion transporters: A result of depolarization and weakening of the bacterial membrane. *J. Med. Chem.* **2015**, *58*, 2358–2366. [[CrossRef](#)]
20. Akhtar, N.; Biswas, O.; Manna, D. Biological applications of synthetic anion transporters. *Chem. Commun.* **2020**, *56*, 14137–14153. [[CrossRef](#)]
21. Valkenier, H.; Judd, L.W.; Li, H.; Hussain, S.; Sheppard, D.N.; Davis, A.P. Preorganized bis-thioureas as powerful anion carriers: Chloride transport by single molecules in large unilamellar vesicles. *J. Am. Chem. Soc.* **2014**, *136*, 12507–12512. [[CrossRef](#)] [[PubMed](#)]
22. Valls, A.; Altava, B.; Aseyev, V.; Carreira-Barral, I.; Conesa, L.; Falomir, E.; García-Verdugo, E.; Luis, S.V.; Quesada, R. Structure-antitumor activity relationships of tripodal imidazolium-amino acid based salts. Effect of the nature of the amino acid, amide substitution and anion. *Org. Biomol. Chem.* **2021**, *19*, 10575–10586. [[CrossRef](#)] [[PubMed](#)]
23. Cai, J.; Sessler, J.L. Neutral CH and cationic CH donor groups as anion receptors. *Chem. Soc. Rev.* **2014**, *43*, 6198–6213. [[CrossRef](#)] [[PubMed](#)]
24. Amendola, V.; Bergamaschi, G.; Boiocchi, M.; Legnani, L.; Lo Presti, E.; Miljkovic, A.; Monzani, E.; Pancotti, F. Chloride-binding in organic-water mixtures: The powerful synergy of C–H donor groups within a bowl-shaped cavity. *Chem. Commun.* **2016**, *52*, 10910–10913. [[CrossRef](#)]

25. Amendola, V.; Boiocchi, M.; Fabbrizzi, L.; Fusco, N. Putting the anion into the cage-fluoride inclusion in the smallest trisimidazolium macrotricyclic. *Eur. J. Org. Chem.* **2011**, *2011*, 6434–6444. [[CrossRef](#)]
26. Amendola, V.; Boiocchi, M.; Colasson, B.; Fabbrizzi, L.; Rodriguez Douton, M.-J.; Ugozzoli, F. A metal-based trisimidazolium cage that provides six C-H hydrogen-bond-donor fragments and includes anions. *Angew. Chem. Int. Ed.* **2006**, *45*, 6920–6924. [[CrossRef](#)]
27. Yoon, J.; Kim, S.K.; Singh, N.J.; Kim, K.S. Imidazolium receptors for the recognition of anions. *Chem. Soc. Rev.* **2006**, *35*, 355–360. [[CrossRef](#)]
28. Chakraborty, D.; Modak, R.; Howlader, P.; Mukherjee, P.S. De novo approach for the synthesis of water-soluble interlocked and non-interlocked organic cages. *Chem. Commun.* **2021**, *57*, 3995–3998. [[CrossRef](#)]
29. Hu, Y.; Long, S.; Fu, H.; She, Y.; Xu, Z.; Yoon, J. Revisiting imidazolium receptors for the recognition of anions: Highlighted research during 2010–2019. *Chem. Soc. Rev.* **2021**, *50*, 589–618. [[CrossRef](#)]
30. Singh, A.; Sharma, S.; Kaur, N.; Singh, N. Self-assembly of imidazolium/benzimidazolium cationic receptors: Their environmental and biological applications. *New J. Chem.* **2020**, *44*, 19360–19375. [[CrossRef](#)]
31. Aletti, A.B.; Miljkovic, A.; Toma, L.; Bruno, R.; Armentano, D.; Gunnlaugsson, T.; Bergamaschi, G.; Amendola, V. Halide-Controlled Extending-Shrinking Motion of a Covalent Cage. *J. Org. Chem.* **2019**, *84*, 4221–4228. [[CrossRef](#)] [[PubMed](#)]
32. Gans, P.; Sabatini, A.; Vacca, A. Investigation of equilibria in solution. Determination of equilibrium constants with the HYPERQUAD suite of programs. *Talanta* **1996**, *43*, 1739–1753. [[CrossRef](#)]
33. Ihm, H.; Yun, S.; Kim, H.G.; Kim, J.K.; Kim, K.S. Tripodal nitro-imidazolium receptor for anion binding driven by (C-H)···X-hydrogen bonds. *Org. Lett.* **2002**, *4*, 2897–2900. [[CrossRef](#)]
34. Zhou, H.; Zhao, Y.; Gao, G.; Li, S.; Lan, J.; You, J. Highly selective fluorescent recognition of sulfate in water by two rigid tetrakisimidazolium macrocycles with peripheral chains. *J. Am. Chem. Soc.* **2013**, *135*, 14908–14911. [[CrossRef](#)] [[PubMed](#)]
35. Sato, K.; Arai, S.; Yamagishi, T. A new tripodal anion receptor with C-H···X⁻ hydrogen bonding. *Tetrahedron Lett.* **1999**, *40*, 5219–5222. [[CrossRef](#)]
36. Li, H.; Valkenier, H.; Thorne, A.G.; Dias, C.M.; Cooper, J.A.; Kieffer, M.; Busschaert, N.; Gale, P.A.; Sheppard, D.N.; Davis, A.P. Anion carriers as potential treatments for cystic fibrosis: Transport in cystic fibrosis cells, and additivity to channel-targeting drugs. *Chem. Sci.* **2019**, *10*, 9663–9672. [[CrossRef](#)] [[PubMed](#)]
37. Li, H.; Valkenier, H.; Judd, L.W.; Brotherhood, P.R.; Hussain, S.; Cooper, J.A.; Jurček, O.; Sparkes, H.A.; Sheppard, D.N.; Davis, A.P. Efficient, non-toxic anion transport by synthetic carriers in cells and epithelia. *Nat. Chem.* **2016**, *8*, 24–32. [[CrossRef](#)] [[PubMed](#)]
38. Cancemi, P.; Buttacavoli, M.; D’Anna, F.; Feo, S.; Fontana, R.M.; Noto, R.; Suter, A.; Vitale, P.; Gallo, G. The effects of structural changes on the anti-microbial and anti-proliferative activities of diimidazolium salts. *New J. Chem.* **2017**, *41*, 3574–3585. [[CrossRef](#)]
39. Marchesi, N.; Barbieri, A.; Fahmideh, F.; Govoni, S.; Ghidoni, A.; Parati, G.; Vanoli, E.; Pascale, A.; Calvillo, L. Use of dual-flow bioreactor to develop a simplified model of nervous-cardiovascular systems crosstalk: A preliminary assessment. *PLoS ONE* **2020**, *15*, e0242627. [[CrossRef](#)]
40. Bassi, B.; Dacarro, G.; Galinetto, P.; Giulotto, E.; Marchesi, N.; Pallavicini, P.; Pascale, A.; Perversi, S.; Taglietti, A. Tailored coating of gold nanostars: Rational approach to prototype of theranostic device based on SERS and photothermal effects at ultralow irradiance. *Nanotechnology* **2018**, *29*, 235301. [[CrossRef](#)]
41. Srivastava, G.K.; Alonso-Alonso, M.L.; Fernandez-Bueno, I.; Garcia-Gutierrez, M.T.; Rull, F.; Medina, J.; Coco, R.M.; Pastor, J.C. Comparison between direct contact and extract exposure methods for PFO cytotoxicity evaluation. *Sci. Rep.* **2018**, *8*, 4525. [[CrossRef](#)] [[PubMed](#)]
42. Weinstein, M.P.; Patel, J.B.; Burnhman, C.-A.; Zimmer, B.L. M07-A Methods for Dilution Antimicrobial Susceptibility Tests for Bacteria that Grow Aerobically. *Clin. Lab. Stand. Inst.* **2012**, *32*, 1–67.
43. Barry, A.L. National Committee for Clinical Laboratory Standards. M26-A Methods for Determining Bactericidal Activity of Antimicrobial Agents; Approved Guideline This document provides procedures for determining the lethal activity of antimicrobial agents. *Clin. Lab. Stand. Inst.* **1999**, *19*, 1–14.
44. Watanabe, G.; Sekiya, H.; Tamai, E.; Saijo, R.; Uno, H.; Mori, S.; Tanaka, T.; Maki, J.; Kawase, M. Synthesis and antimicrobial activity of 2-trifluoroacetylbenzoxazole ligands and their metal complexes. *Chem. Pharm. Bull.* **2018**, *66*, 732–740. [[CrossRef](#)]
45. Brusotti, G.; Cesari, I.; Frassà, G.; Grisoli, P.; Dacarro, C.; Caccialanza, G. Antimicrobial properties of stem bark extracts from *Phyllanthus muellerianus* (Kuntze) Excell. *J. Ethnopharmacol.* **2011**, *135*, 797–800. [[CrossRef](#)] [[PubMed](#)]
46. D’Agostino, A.; Taglietti, A.; Desando, R.; Bini, M.; Patrini, M.; Dacarro, G.; Cucca, L.; Pallavicini, P.; Grisoli, P. Bulk surfaces coated with triangular silver nanoplates: Antibacterial action based on silver release and photo-thermal effect. *Nanomaterials* **2017**, *7*, 7. [[CrossRef](#)]
47. Toci, G.; Olgiati, F.; Pallavicini, P.; Fernandez, Y.A.D.; De Vita, L.; Dacarro, G.; Grisoli, P.; Taglietti, A. Gold nanostars embedded in PDMS films: A photothermal material for antibacterial applications. *Nanomaterials* **2021**, *11*, 3252. [[CrossRef](#)]
48. Perugini, P.; Bonetti, M.; Guerini, M.; Musitelli, G.; Grisoli, P. A New In Vitro Model to Evaluate Anti-Adhesive Effect against Fungal Nail Infections. *Appl. Sci.* **2021**, *11*, 1977. [[CrossRef](#)]
49. Amato, E.; Diaz-Fernandez, Y.A.; Taglietti, A.; Pallavicini, P.; Pasotti, L.; Cucca, L.; Milanese, C.; Grisoli, P.; Dacarro, C.; Fernandez-Hechavarria, J.M.; et al. Synthesis, Characterization and Antibacterial Activity against Gram Positive and Gram Negative Bacteria of Biomimetically Coated Silver Nanoparticles. *Langmuir* **2011**, *27*, 9165–9173. [[CrossRef](#)]
50. *CrysAlisPro*, 1.171.38.41; Rigaku Oxford Diffraction; Rigaku: Oxfordshire, UK, 2015.

51. Evans, P. Scaling and Assessment of Data Quality. *Acta Crystallogr. Sect. D Biol. Crystallogr.* **2006**, *62*, 72–82. [[CrossRef](#)]
52. Evans, P.R.; Murshudov, G.N. How Good Are My Data and What Is the Resolution? *Acta Crystallogr. Sect. D Biol. Crystallogr.* **2013**, *69*, 1204–1214. [[CrossRef](#)] [[PubMed](#)]
53. Winn, M.D.; Ballard, C.C.; Cowtan, K.D.; Dodson, E.J.; Emsley, P.; Evans, P.R.; Keegan, R.M.; Krissinel, E.B.; Leslie, A.G.W.; McCoy, A.; et al. Overview of the CCP 4 Suite and Current Developments. *Acta Crystallogr. Sect. D Biol. Crystallogr.* **2011**, *67*, 235–242. [[CrossRef](#)] [[PubMed](#)]
54. Winter, G. An Expert System for Macromolecular Crystallography Data Reduction. *J. Appl. Crystallogr.* **2010**, *43*, 186–190. [[CrossRef](#)]
55. Sheldrick, G.M. Crystal Structure Refinement with SHELXL. *Acta Crystallogr. Sect. C Struct. Chem.* **2015**, *71*, 3–8. [[CrossRef](#)]
56. Sheldrick, G.M. A Short History of SHELX. *Acta Crystallogr. A.* **2008**, *64*, 112–122. [[CrossRef](#)]
57. Spek, A.L. Structure Validation in Chemical Crystallography. *Acta Crystallogr. D. Biol. Crystallogr.* **2009**, *65*, 148–155. [[CrossRef](#)]
58. Farrugia, L.J. WinGX Suite for Small-Molecule Single-Crystal Crystallography. *J. Appl. Crystallogr.* **1999**, *32*, 837–838. [[CrossRef](#)]
59. Palmer, D.C. *Crystalmaker*; CrystalMaker Software Ltd: Oxfordshire, UK, 2014.